

# Photoinduced sign inversion of the anomalous Hall effect in EuO thin films

Y. Ohuchi,<sup>1</sup> Y. Kozuka,<sup>1,\*</sup> N. Rezaei,<sup>2</sup> M. S. Bahramy,<sup>1,3</sup> R. Arita,<sup>1,4</sup> K. Ueno,<sup>4,5</sup> A. Tsukazaki,<sup>4,6</sup> and M. Kawasaki<sup>1,3</sup>

<sup>1</sup>*Department of Applied Physics and Quantum-Phase Electronics Center (QPEC), University of Tokyo, Tokyo 113-8656, Japan*

<sup>2</sup>*Department of Physics, Isfahan University of Technology, Isfahan 84154, Iran*

<sup>3</sup>*Center for Emergent Matter Science (CEMS), RIKEN, Wako, Saitama 351-0198, Japan*

<sup>4</sup>*PRESTO, Japan Science and Technology Agency (JST), Chiyoda-ku, Tokyo 102-0075, Japan*

<sup>5</sup>*Department of Basic Science, University of Tokyo, Tokyo 153-8902, Japan*

<sup>6</sup>*Institute for Materials Research, Tohoku University, Sendai 980-8577, Japan*

(Received 27 October 2013; revised manuscript received 26 February 2014; published 26 March 2014)

We report on the sign inversion of the anomalous Hall effect (AHE) in EuO thin films along with photoirradiation as well as a temperature scan across  $\sim 25$  K that is well below the Curie temperature ( $T_C \sim 80$  K). The former gives an enhancement of the mobile electron density ( $n$ ) by more than 30%, but the latter gives a negligible modification of  $n$  of only 3% with a significant enhancement in mobility. It is found, in addition to the universal scaling law between longitudinal conductivity ( $\sigma_{xx}$ ) and anomalous Hall conductivity ( $\sigma_{AH}$ ) as  $|\sigma_{AH}| \propto \sigma_{xx}^{1.6}$ , that there is a critical value of about  $10^2$  S cm<sup>-1</sup> in  $\sigma_{xx}$  that gives a boundary in the sign inversion of  $\sigma_{AH}$ . If  $n$  solely governs the sign of  $\sigma_{AH}$ , the phenomenon could be explained by a Fermi level shift across the singularity in the band structure. However, our band calculation shows that, within any realistic adjustment of band parameters, the sign inversion of AHE never occurs. Thus, we conclude that other mechanisms of AHE are necessary to account for the AHE of EuO.

DOI: [10.1103/PhysRevB.89.121114](https://doi.org/10.1103/PhysRevB.89.121114)

PACS number(s): 75.50.Pp, 73.50.Pz, 71.20.Nr, 81.05.Hd

Controlling the spin degrees of freedom of electrons in a solid is one of the main courses to realize new devices with nonvolatility, high density, and low power consumption [1,2]. Magnetic semiconductors are an important class of materials in this field because of the controllability of physical properties by a variety of external stimuli, such as electric and magnetic fields as well as by chemical doping. Among them, EuO is one of the most prototypical and well-studied ferromagnetic semiconductors. While undoped EuO is an insulator with a band gap of  $\sim 1.2$  eV across the Eu 4*f*-Eu 5*d* transition [3], chemical doping of a trivalent element or an oxygen deficiency injects mobile electrons in the conduction band [4]. This chemical doping enables us to enhance the ferromagnetic transition temperature ( $T_C$ ) from 70 to 200 K, depending on the carrier density. The characteristic properties of EuO are large magnetoresistive [5,6] and magneto-optical effects [7–11], which make this material appealing for electric and optical applications. Another fundamental physical property of electron-doped EuO is the anomalous Hall effect (AHE) [12]. Although AHE is one of the important physical properties of magnetic metals and semiconductors [13], only recently has AHE of EuO been observed in thin films [12], on which we focus in this Rapid Communication.

The theories of AHE have been rapidly developed during the past decade beyond the conventional extrinsic mechanisms such as skew scattering [14] and side jumps [15], which require magnetic impurities interacting with conducting electrons. Contemporary theories can explain the complex behaviors of AHE without employing magnetic impurities. There are mainly two categories: one taking into account the band structure in momentum space [16,17] and the other based on nontrivial spin structures in real space [18–20]. In the former,

band crossing near the Fermi level ( $E_F$ ) acts as a magnetic monopole, generating an anomalous Hall velocity as a result of a spin-orbit interaction. This theory has successfully explained the sign inversion of AHE in several itinerant ferromagnets such as SrRuO<sub>3</sub> [17], (La,Eu)TiO<sub>3</sub> [21], and Mn-doped GaAs [22,23] in response to the  $E_F$  shift across the band crossing point. In the other theory, itinerant electrons gain a phase factor when hopping in a noncollinear spin background. Since a nontrivial spin structure is necessary, this theory has been applied to materials, for example, with frustrated spin systems [19] or with skyrmion crystals [24]. In comparison with these magnetic metals and semiconductors, however, AHE of EuO has not been well studied in detail.

In this Rapid Communication, we report on the sign inversion of AHE in moderately oxygen deficient EuO epitaxial thin films. We find this phenomenon can be triggered by photoirradiation as well as by a temperature variation. As opposed to the aforementioned theory, a band calculation indicates that there is no band crossing near  $E_F$  and therefore sign inversion is not expected. This fact necessitates another scenario to account for the AHE in this material.

The details of the growth conditions are described in Ref. [12]. Briefly, EuO epitaxial films were fabricated on YAlO<sub>3</sub> (110) substrates by pulsed laser deposition at 300 °C using a Eu metal target under  $1 \times 10^{-5}$  Torr of Ar gas containing 1% O<sub>2</sub>. We used KrF excimer laser pulses for the deposition at a repetition of 15 Hz. We deposited a 50-nm-thick EuO film followed by a 2-nm AlO<sub>x</sub> capping layer deposited *in situ* at room temperature in order to avoid oxidization of Eu<sup>2+</sup> in air. The film was patterned into a Hall bar by photolithography and Ar ion etching for transport measurements. A Hg-Xe lamp was used for the photoconductivity measurement with the total intensity ranging from  $3.6 \times 10^{-6}$  to  $5.5 \times 10^{-3}$  W/cm<sup>2</sup> in this measurement. Due to the absence of filtering, the light contains a broad wavelength with an energy range of 1.6–5.0 eV. The Hall resistivity was analyzed by

\*Author to whom correspondence should be addressed: kozuka@ap.t.u-tokyo.ac.jp

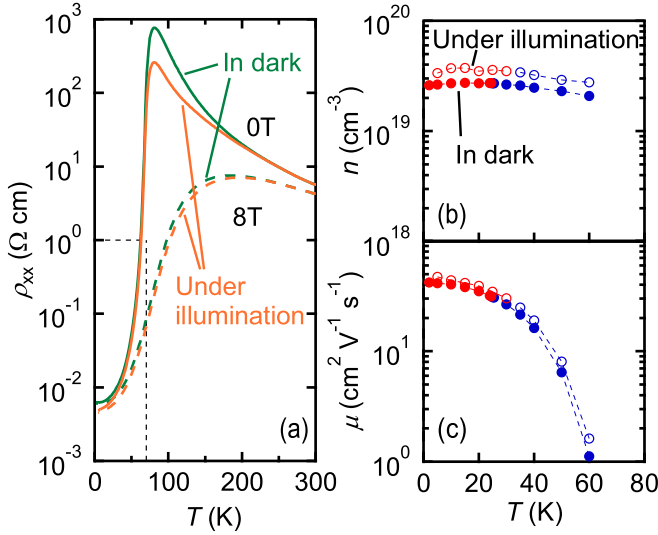


FIG. 1. (Color online) (a) Temperature ( $T$ ) dependence of resistivity ( $\rho_{xx}$ ) in the dark (green) and under illumination (orange) at  $B = 0 \text{ T}$  (solid curve) and  $8 \text{ T}$  (dotted curve). The box with dashed lines is the region magnified in Fig. 4(a).  $T$  dependence of (b) carrier density ( $n$ ) and (c) mobility ( $\mu$ ) below  $60 \text{ K}$ . Solid circles represent the data in the dark and open circles under illumination. The sign of the anomalous Hall conductivity ( $\sigma_{\text{AH}}$ ), which will be discussed in Fig. 2, is classified by colors as blue and red symbols for negative and positive signs, respectively.

antisymmetrizing the raw Hall resistivity data ( $\rho_{xy}^{\text{raw}}$ ) to exclude the contribution from longitudinal magnetoresistance as  $\rho_{xy}(B) = [\rho_{xy}^{\text{raw}}(B) - \rho_{xy}^{\text{raw}}(-B)]/2$ , where the sweep direction of  $B$  is opposite between  $\rho_{xy}^{\text{raw}}(B)$  and  $\rho_{xy}^{\text{raw}}(-B)$  to ensure the opposite magnetization direction.

First of all, we show the basic transport characteristics together with the effect of photoirradiation. Figure 1(a) shows the temperature dependence of resistivity ( $\rho_{xx}$ ) in the dark (green) and under illumination with the highest intensity (orange) at  $B = 0 \text{ T}$  (solid curve) and  $8 \text{ T}$  (dotted curve). Without an external magnetic field,  $\rho_{xx}$  shows a transition from insulating to metallic behavior around  $80 \text{ K}$  while cooling, which is associated with the ferromagnetic transition. With applying a magnetic field,  $\rho_{xx}$  is dramatically suppressed with the ratio of  $\rho_{xx}(8 \text{ T})/\rho_{xx}(0 \text{ T})$  reaching below  $2.3 \times 10^{-4}$  at  $76 \text{ K}$ . This behavior is qualitatively the same as that of previously reported carrier doped EuO thin films [6,12]. We then irradiated the film to investigate photoconductivity [25,26]. While  $\rho_{xx}$  does not significantly reduce above  $200 \text{ K}$ , photoconductivity is pronounced at lower temperatures. At  $81 \text{ K}$ , the  $\rho_{xx}$  reduces by 66% at maximum. Nevertheless, the temperature giving the resistance peak does not change much with photoirradiation, probably due to an insufficient amount of photoinduced carriers to cause the enhancement of  $T_C$ . Figures 1(b) and 1(c) show the temperature dependence of electron density ( $n$ ) and mobility ( $\mu$ ), respectively, below  $60 \text{ K}$ . The former was calculated from the ordinary term of the Hall effect, which is the field gradient of antisymmetrized Hall resistivity at a high field ( $B > 5 \text{ T}$ ) where sample magnetization is fully saturated [12]. Photoirradiation certainly increased  $n$  while  $\mu$  increased to a lesser degree. In contrast,  $\mu$  dominantly

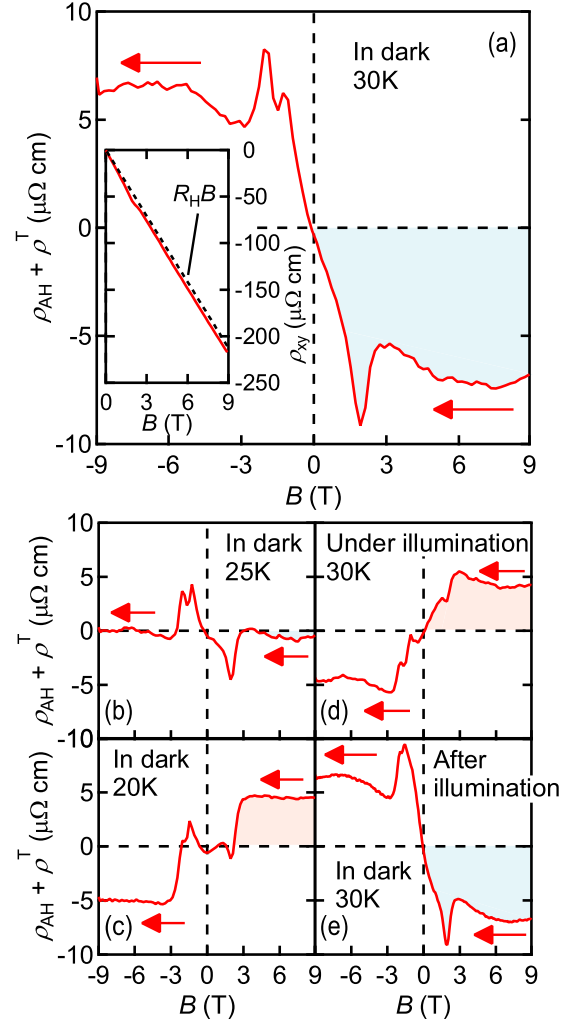


FIG. 2. (Color online) Magnetic field ( $B$ ) dependence of non-ordinary Hall resistivity ( $\rho_{xy} - R_H B$ ) defined by Eq. (1) in the dark at (a) 30, (b) 25, and (c) 20 K. Reversible effects of illumination are shown by those at 30 K (d) under illumination and (e) in the dark after switching off the illumination. The illumination intensity was  $5.5 \times 10^{-3} \text{ W/cm}^2$  in this study. The inset of (a) shows the  $B$  dependence of Hall resistivity ( $\rho_{xy}$ ) at 30 K. The black dashed line in the inset displays a slope of the ordinary Hall effect ( $R_H B$ ). The blue and red regions correspond to negative and positive signs of  $\sigma_{\text{AH}}$ , respectively. The arrows indicate the field scan direction.

varies with temperature, while  $n$  is almost constant over the temperature range as investigated.

We then investigated AHE by varying the temperature and intensity of photoirradiation. The Hall resistivity is expressed as

$$\rho_{xy} = R_H B + \rho_{\text{AH}} + \rho^T, \quad (1)$$

where  $R_H$  is the ordinary Hall coefficient and the rest which includes the conventional anomalous Hall term ( $\rho_{\text{AH}}$ ) proportional to magnetization ( $M$ ) and the additional nonordinary (topological) term ( $\rho^T$ ) generated by a nontrivial spin texture and appearing as a peak structure at a field just before the saturation [12,27]. Figure 2(a) shows the magnetic field dependence of the Hall resistivity ( $\rho_{\text{AH}} + \rho^T$ ) in the dark at

30 K after subtracting the  $B$ -linear high-field ordinary term from  $\rho_{xy}$  [Eq. (1)], for which the original data are shown in the inset. At this temperature,  $\rho_{AH}$  proportional to  $M$  showed a negative value as in a previous report [12]. With decreasing temperature,  $\rho_{AH}$  became nearly zero at 25 K [Fig. 2(b)], and eventually the sign was inverted to a positive value at 20 K [Fig. 2(c)]. To further examine this phenomenon, the light was irradiated at 30 K. As a consequence, we did observe the sign inversion of AHE under illumination, as shown in Fig. 2(d). With the light switched off,  $\rho_{AH}$  returned to the original sign with nearly the same absolute value [Fig. 2(e)], from which we confirmed the intrinsic effect of the photoconductivity rather than some irreversible processes such as the creation of oxygen vacancies. It is also worth noting that this photoinduced sign inversion is not a result of heating by light illumination because the temperature increase always gives a negative sign in AHE above 30 K.

We now consider the origin of the sign inversion in the AHE within the framework of the aforementioned theories. First of all, conventional theories incorporating an extrinsic effect dictate  $\rho_{AH} \approx \rho_{xx}^\beta$  with  $\beta = 1$  in the case of skew scattering and  $\beta = 2$  in the case of a side-jump mechanism. However, both  $\beta$  values are not consistent with the experimental  $\beta$  value of  $\sim 0.4$ , as will be discussed later. Moreover, these theories cannot account for the sign inversion within the standard formalism [13,15]. The topological term in Eq. (1) also cannot be the primary origin because this contribution is not significant at magnetic fields that are much higher than the magnetization saturation ( $\sim 3$  T). Therefore, we were prompted to explain the sign inversion of the AHE by the  $E_F$  shift across the singularity point of the band structure as this theory has been successful in explaining the sign inversion of AHE by  $E_F$  tuning in many cases, such as (La,Eu)TiO<sub>3</sub> or Mn-doped GaAs [21,22]. In order to theoretically access this consideration, we carried out relativistic electronic structure calculations within the context of density functional theory using the Perdew-Burke-Ernzerhof (PBE) exchange-correlation functional [28] and the augmented plane wave plus atomic orbitals method as implemented in the WIEN2K program [29]. The atomic muffin-tin radii  $R_{MT}$  and maximum modulus of reciprocal vectors  $K_{max}$  were chosen such that  $R_{MT}K_{max} = 7$ . The lattice parameters and atomic parameters were taken from experiment [30] and the corresponding Brillouin zone was sampled by a  $10 \times 10 \times 10$   $k$  mesh. The anomalous Hall conductivity was calculated using a set of maximally localized Wannier functions [31], constructed from WIEN2K calculations [32,33].

Figure 3(a) shows the band structure of EuO as obtained from the PBE calculations with the inclusion of the on-site Hubbard  $U$  and exchange  $J$  parameters as well as a spin-orbit interaction. We assume  $U - J = 7$  eV [34]. The color expresses the  $z$ -component projection of spins. The obtained band structure indicates that the conduction band mainly consists of Eu 5d orbitals, while the localized 4f states form the valence band, qualitatively consistent with that of previous calculations carried out in the absence of a spin-orbit interaction [34,35]. As clearly shown in the band structure, there is no singularity around the bottom of the conduction band. The anomalous Hall conductivity, calculated based

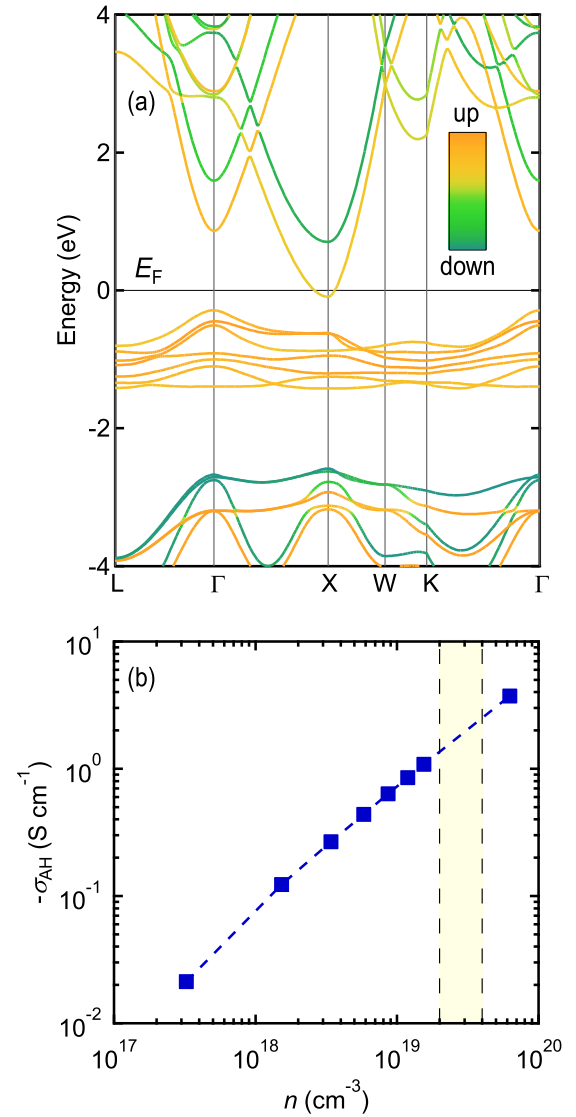


FIG. 3. (Color online) (a) Energy band calculation of EuO including the on-site Coulomb interaction ( $U = 7$  eV) and the spin-orbit interaction. The color code indicates the  $z$ -component projection of spins. (b) Anomalous Hall conductivity as a function of carrier density. Squares are results calculated from the band structure of (a) and the range of the carrier density in this experiment is colored as yellow.

on the band structure without including disorder following Ref. [36], shows a monotonic variation without any indication of sign inversion [Fig. 3(b)]. This result is clearly inconsistent with our considerations based on the  $E_F$  shift.

In fact, Fig. 1(b), where the sign of AHE is categorized by color, implies that the carrier density, and hence  $E_F$  shift, alone cannot account for the sign inversion. Under the light illumination, the carrier density increased by 32% at 30 K, where the sign of AHE is inverted by photoconductivity. On the other hand, by comparing the carrier density between 30 and 20 K in the dark, where the sign of AHE is inverted by a temperature variation, the increase of the carrier is only 3%

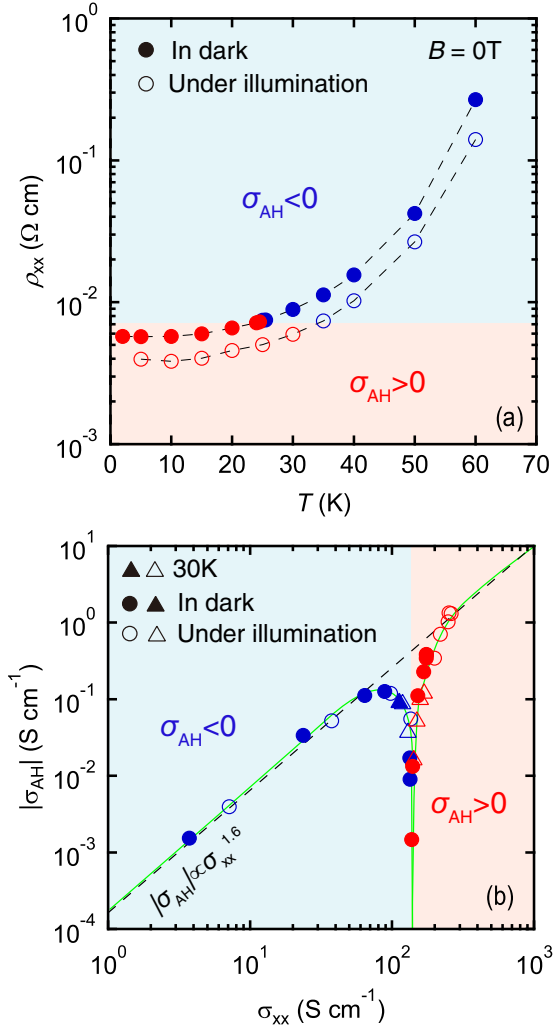


FIG. 4. (Color online) (a)  $T$  dependence of  $\rho_{xx}$  below 60 K at  $B = 0$  T. Solid and open circles are the data taken in the dark and under illumination, respectively. Those in blue and red, respectively, represent the negative and positive signs of the anomalous Hall conductivity ( $\sigma_{AH}$ ). The dashed curves are guides to the eyes. (b) The data are plotted in the relationship between the longitudinal conductivity at  $B = 0$  T ( $\sigma_{xx}$ ) and the absolute value of the anomalous Hall conductivity at 9 T ( $|\sigma_{AH}|$ ). Triangles represent the data at 30 K under illumination with a variety of light intensities spanning two orders of magnitude. The dashed line indicates  $|\sigma_{AH}| \propto \sigma_{xx}^{1.6}$ . The green curve is a guide to the eyes.

from 30 to 20 K. Based on these facts, it is not reasonable to regard the sign of AHE as a function of carrier density. Rather, this sign change may well be correlated with the resistivity value, which is plotted in Fig. 4(a). The separatrix (the boundary between the red and blue regions) in resistivity to cause the sign inversion resides around  $7.3 \times 10^{-3} \Omega \text{ cm}$ .

In this respect, we compared the experimental values with the theory by Karplus *et al.* [16] by incorporating the effects of disorder. While  $\sigma_{AH}$  is constant in the clean limit, a scaling relation as  $|\sigma_{AH}| \propto \sigma_{xx}^{1.6}$  follows with increasing disorder, where  $\sigma_{xx} = 1/\rho_{xx}$  is the longitudinal conductivity at  $B = 0$  T and  $\sigma_{AH} = (\rho_{AH} + \rho^T)/[\rho_{xx}^2 + (\rho_{AH} + \rho^T)^2]$  is the anomalous Hall conductivity at 9 T [37,38]. Figure 4(b)

shows  $|\sigma_{AH}|$  as a function of  $\sigma_{xx}$ . The relation  $|\sigma_{AH}| \propto \sigma_{xx}^{1.6}$  (corresponding to  $\rho_{AH} \sim \rho_{xx}^{0.4}$  with setting  $\rho^T = 0$  at 9 T and with neglecting  $\rho_{AH}$  in the denominator) holds well for all the data investigated, irrespective of the sign of  $\sigma_{AH}$  except those around the sign inversion yielding a sharp cusp at  $\sigma_{xx}$  of about  $10^2 \text{ S cm}^{-1}$ , which indicates the  $\sigma_{xx}$  is in a dirty regime. We also note that, whether  $\sigma_{xx}$  varies by temperature or by light illumination,  $|\sigma_{AH}|$  traces a single curve including the cusp region.

Although the above phenomenological consideration suggests that disorder is in reality effective in EuO thin films, the microscopic mechanism is not yet clear at the moment. Given the simple conduction band structure of EuO shown in Fig. 3(a), there may be other mechanisms that causes sign reversal in AHE. As a possibility, when multiple contributions compete with each other, a subtle variation of these could cause the sign inversion. However, even if we assume that, for instance, the intrinsic mechanism and side jump nearly cancel each other out, the steep rise of  $\sigma_{AHE}$  (reaching 1 S/cm) across the sign inversion is unlikely to appear since both contributions cannot vary so rapidly below 30 K due to the small variation of all material parameters, including conductivity and magnetization.

Thus all the above considerations based on the existing theories seem to fail to explain the sign inversion of AHE in EuO thin films. In this respect, it may be important to extract a possible key ingredient by including other material systems showing the sign inversion by a temperature variation or by  $E_F$  tuning, namely, SrRuO<sub>3</sub> [17], La-doped EuTiO<sub>3</sub> [21], and Mn-doped GaAs [22]. Here we note that these studies have been performed in thin film forms with thicknesses below  $\sim 50$  nm, whereas the sign inversion of AHE has hardly been reported in bulk materials. However, the explanations solely rely on the Berry-phase scenario based on bulk electronic structures. In fact, this approach is not always valid as thick Mn-doped GaAs films do not show the sign inversion even with a conductivity range that is similar to the thin samples, which the authors attributed to the unknown effects of reduced dimensionality and disorder [22]. Similar but unrevealed effects such as modified electronic or magnetic structures at the surface or interface could play a significant role in the case of the EuO thin film as well. Under the irradiation, the redistribution of conducting electrons in the film may additionally trigger the sign inversion of AHE.

As another possibility, we could postulate a situation that is characteristic in EuO. Recent studies on angle-resolved photoemission spectroscopy of EuO have revealed its unique electronic structure, which showed deeply bounded states at the  $\Gamma$  point in the ferromagnetic phase [39]. Although they are likely to be defect derived and almost no contribution is made to  $\sigma_{xx}$ , we speculate that the Berry phase generated from these bounded states could influence the inversion of the sign of AHE. In this case, the additional states  $|n, \mathbf{k}\rangle$  should be also included in the Berry-phase connection  $\mathbf{a}_n = i \langle n, \mathbf{k} | \nabla_{\mathbf{k}} | n, \mathbf{k} \rangle$  to calculate  $\sigma_{AH}$  [13]. To fully understand the observation, further studies are needed.

In conclusion, we have observed the sign inversion of the AHE in EuO thin films by photodoping as well as by temperature variation. This behavior cannot be explained based on the anomalous Hall velocity arising from a band crossing



point, as well as on other existing theories, and remains to be investigated both from theoretical and experimental viewpoints.

We thank T. Fukumura for allowing us to use the Hg-Xe light source and M. Uchida and D. Chiba for helpful

discussions. This work was supported in part by a JSPS Grant-in-Aid for Scientific Research(S) No. 24226002 Japan, and by “Funding Program for World-Leading Innovative R&D on Science and Technology (FIRST)” Program from the Japan Society for the Promotion of Science (JSPS), initiated by the Council for Science and Technology Policy.

- 
- [1] I. Žutić, J. Fabian, and S. D. Sarma, *Rev. Mod. Phys.* **76**, 323 (2004).
  - [2] D. D. Awschalom and M. E. Flatté, *Nat. Phys.* **3**, 153 (2007).
  - [3] A. Mauger and C. Godart, *Phys. Rep.* **141**, 51 (1986).
  - [4] H. Miyazaki, H. J. Im, K. Terashima, S. Yagi, M. Kato, K. Soda, T. Ito, and S. Kimura, *Appl. Phys. Lett.* **96**, 232503 (2010).
  - [5] Y. Shapira, S. Foner, and T. B. Reed, *Phys. Rev. B* **8**, 2299 (1973).
  - [6] A. Schmehl, V. Vaithyanathan, A. Herrnberger, S. Thiel, C. Richter, M. Liberati, T. Heeg, M. Röckerath, L. F. Kourkoutis, S. Mühlbauer, P. Boni, D. A. Muller, Y. Barash, J. Schubert, Y. Idzerda, J. Mannhart, and D. G. Schlom, *Nat. Mater.* **6**, 882 (2007).
  - [7] K. Y. Ahn and J. C. Suits, *IEEE Trans. Magn.* **3**, 453 (1967).
  - [8] M. Matsubara, A. Schmehl, J. Mannhart, D. G. Schlom, and M. Fiebig, *Phys. Rev. B* **81**, 214447 (2010).
  - [9] M. Matsubara, A. Schmehl, J. Mannhart, D. G. Schlom, and M. Fiebig, *Phys. Rev. B* **86**, 195127 (2012).
  - [10] T. Makino, F. Liu, T. Yamasaki, Y. Kozuka, K. Ueno, A. Tsukazaki, T. Fukumura, Y. Kong, and M. Kawasaki, *Phys. Rev. B* **86**, 064403 (2012).
  - [11] F. Liu, T. Makino, T. Yamasaki, K. Ueno, A. Tsukazaki, T. Fukumura, Y. Kong, and M. Kawasaki, *Phys. Rev. Lett.* **108**, 257401 (2012).
  - [12] T. Yamasaki, K. Ueno, A. Tsukazaki, T. Fukumura, and M. Kawasaki, *Appl. Phys. Lett.* **98**, 082116 (2011).
  - [13] N. Nagaosa, J. Sinova, S. Onoda, A. H. MacDonald, and N. P. Ong, *Rev. Mod. Phys.* **82**, 1539 (2010).
  - [14] J. Smit, *Physica* **24**, 39 (1958).
  - [15] L. Berger, *Phys. Rev. B* **2**, 4559 (1970).
  - [16] R. Karplus and J. M. Luttinger, *Phys. Rev.* **95**, 1154 (1954).
  - [17] Z. Fang, N. Nagaosa, K. S. Takahashi, A. Asamitsu, R. Mathieu, T. Ogasawara, H. Yamada, M. Kawasaki, Y. Tokura, and K. Terakura, *Science* **302**, 92 (2003).
  - [18] K. Ohgushi, S. Murakami, and N. Nagaosa, *Phys. Rev. B* **62**, R6065 (2000).
  - [19] Y. Taguchi, Y. Oohara, H. Yoshizawa, N. Nagaosa, and Y. Tokura, *Science* **291**, 2573 (2001).
  - [20] T. Tomizawa and H. Kontani, *Phys. Rev. B* **82**, 104412 (2010).
  - [21] K. S. Takahashi, M. Onoda, M. Kawasaki, N. Nagaosa, and Y. Tokura, *Phys. Rev. Lett.* **103**, 057204 (2009).
  - [22] D. Chiba, A. Werpachowska, M. Endo, Y. Nishitani, F. Matsukura, T. Dietl, and H. Ohno, *Phys. Rev. Lett.* **104**, 106601 (2010).
  - [23] A. A. Kovalev, J. Sinova, and Y. Tserkovnyak, *Phys. Rev. Lett.* **105**, 036601 (2010).
  - [24] A. Neubauer, C. Pfleiderer, B. Binz, A. Rosch, R. Ritz, P. G. Niklowitz, and P. Böni, *Phys. Rev. Lett.* **102**, 186602 (2009).
  - [25] R. Bachmann and P. Wachter, *Solid State Commun.* **6**, 711 (1968).
  - [26] C. Llinares, L. Gousskov, C. Duchemin, and G. Bordure, *J. Phys. Chem. Solids* **36**, 567 (1975).
  - [27] N. Kanazawa, Y. Onose, T. Arima, D. Okuyama, K. Ohoyama, S. Wakimoto, K. Kakurai, S. Ishiwata, and Y. Tokura, *Phys. Rev. Lett.* **106**, 156603 (2011).
  - [28] J. P. Perdew, K. Burke, and M. Ernzerhof, *Phys. Rev. Lett.* **77**, 3865 (1996).
  - [29] P. Blaha, K. Schwarz, G. Madsen, D. Kvasnicka, and J. Luitz, WIEN2K package, available at <http://www.wien2k.at>
  - [30] D. Taylor, *Trans. J. Br. Ceram. Soc.* **83**, 5 (1984).
  - [31] I. Souza, N. Marzari, and D. Vanderbilt, *Phys. Rev. B* **65**, 035109 (2001).
  - [32] A. A. Mostofi, J. R. Yates, Y.-S. Lee, I. Souza, D. Vanderbilt, and N. Marzari, *Comput. Phys. Commun.* **78**, 685 (2008).
  - [33] J. Kunes, R. Arita, P. Wissgott, A. Toschi, H. Ikeda, and K. Held, *Comput. Phys. Commun.* **181**, 1888 (2010).
  - [34] S. J. Cho, *Phys. Rev. B* **1**, 4589 (1970).
  - [35] H. Miyazaki, T. Ito, H. J. Im, S. Yagi, M. Kato, K. Soda, and S. Kimura, *Phys. Rev. Lett.* **102**, 227203 (2009).
  - [36] X. Wang, J. R. Yates, I. Souza, and D. Vanderbilt, *Phys. Rev. B* **74**, 195118 (2006).
  - [37] S. Onoda, N. Sugimoto, and N. Nagaosa, *Phys. Rev. Lett.* **97**, 126602 (2006).
  - [38] T. Fukumura, H. Toyosaki, K. Ueno, M. Nakano, T. Yamasaki, and M. Kawasaki, *Jpn. J. Appl. Phys.* **46**, L642 (2007).
  - [39] D. E. Shai, A. J. Melville, J. W. Harter, E. J. Monkman, D. W. Shen, A. Schmehl, D. G. Schlom, and K. M. Shen, *Phys. Rev. Lett.* **108**, 267003 (2012).